

PIC Simulations of the Dayside Magnetopause: Origins and Evolution of the Electron and Ion Populations in its Boundary Layers

Jean Berchem¹, Giovanni Lapenta², Robert Richard¹, William Paterson³, and C Philippe Escoubet⁴

¹University of California Los Angeles

²Katholieke Universiteit Leuven

³NASA Goddard Space Flight Center

⁴ESTEC/ESA

November 24, 2022

Abstract

Recent observations and simulations have revealed a wide variety of plasma processes and multiscale structures at the dayside magnetopause. In this presentation, we focus on the origins and evolution of the plasma populations observed in the magnetopause boundary layers. We present the results of Particle-In-Cell (PIC) simulations encompassing large volumes of the dayside magnetosphere. The implicit PIC code used in the study was initialized from a global MHD state of the magnetosphere for southward interplanetary field conditions. Three-dimensional plots of the perpendicular slippage indicates that reconnection occurs over most of the dayside magnetopause. However, the simulation reveals that the reconnection region has a much more filamentary structure than the X-line expected from the extrapolation of 2D models and that multiscale structures thread the reconnection outflow. In particular, the simulation indicates the formation of multiple layers of electrons with significant field-aligned velocities within the main magnetopause current layer. We use velocity distribution functions at different locations in the reconnection outflow to characterize the origins and evolution of the electron and ion populations of the magnetosheath and magnetospheric boundary layers.

PIC Simulations of the Dayside Magnetopause: Origins and Evolution of the Electron and Ion Populations in its Boundary Layers

Jean Berchem (1), Giovanni Lapenta (2), Robert L. Richard (1), William R. Paterson (3), C. Philippe Escoubet (4)

(1) Department of Physics and Astronomy, UCLA, Los Angeles, California, USA

(2) Centre for Plasma Astrophysics KU, Leuven, Belgium

(3) NASA Goddard Space Flight Center, Greenbelt, Maryland, USA

(4) ESA ESTEC, Noordwijk, Netherlands

Abstract: Recent observations and simulations have revealed a wide variety of plasma processes and multiscale structures at the dayside magnetopause. In this presentation, we focus on the origins and evolution of the plasma populations observed in the magnetopause boundary layers. We present the results of Particle-In-Cell (PIC) simulations encompassing large volumes of the dayside magnetosphere. The implicit PIC code used in the study was initialized from a global MHD state of the magnetosphere for southward interplanetary field conditions. Three-dimensional plots of the perpendicular slippage indicates that reconnection occurs over most of the dayside magnetopause. However, the simulation reveals that the reconnection region has a much more filamentary structure than the X-line expected from the extrapolation of 2D models and that multiscale structures thread the reconnection outflow. In particular, the simulation indicates the formation of multiple layers of electrons with significant field-aligned velocities within the main magnetopause current layer. We use velocity distribution functions at different locations in the reconnection outflow to characterize the origins and evolution of the electron and ion populations of the magnetosheath and magnetospheric boundary layers.

Introduction

- Recent observations from Cluster and MMS have revealed a wide variety of plasma processes and multiscale structures at Earth's dayside magnetopause.
- By determining the origins, evolution, and interactions of the plasma populations and electromagnetic structures observed in the reconnection outflows, we can better understand the impact of magnetic reconnection on the structure and dynamics of the magnetopause and assess energy conversion.
- In this presentation, we focus on the origins and evolution of the plasma populations observed in the sunward layer adjacent to the MP, the magnetosheath boundary layer (MSBL) and in its earthward layer, the low-latitude boundary layer (LLBL) that make up the reconnection outflow (see **Figure 1**) as expected from a simple open magnetosphere model [e.g. Cowley, 1980].

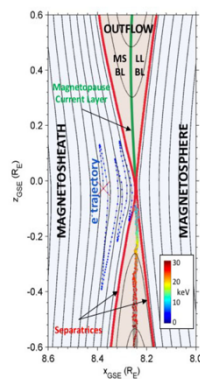


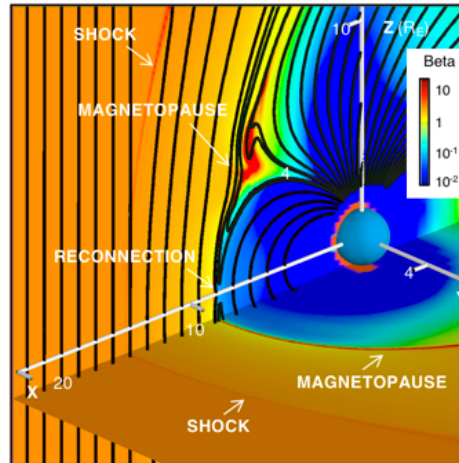
Figure 1: Outflow regions from an iPic3D simulation. The Large Scale Kinetic trajectory of an electron, color coded by energy, shows that it gains a significant amount of energy without passing through the diffusion region.

- Establishing a comprehensive view of the complex physics of the outflow regions is challenging. Most of the existing PIC models are constrained to small physical domains centered on the diffusion regions and/or to 2D geometries.
- To address this problem, we use a 3D implicit PIC code (iPic3D) that is initialized from the results of a global MHD simulation of the solar wind interaction with the magnetosphere-ionosphere system for a southward interplanetary magnetic field (IMF) conditions.
- Our multiscale model includes both the structure (e.g. asymmetries, MP curvature, magnetic cusps) and the dynamics resulting from large-scale magnetospheric fields and plasma stresses, while at the same time resolving local dynamics down to the electron scale.
- The regional PIC simulations encompass a large volume of the dayside magnetosphere ($7 \times 12 \times 12 R_E$) centered on the subsolar magnetopause.

Model and Large-Scale Topology

Global MHD Simulation: Initial Conditions

- **No dipole tilt**
- **Ionosphere:**
 - constant conductance: $\sigma_H = 0$; $\sigma_P = 5$ S
 - no sunlight contribution
- **High-resolution grid:**
 - $\delta x = 0.025 R_E \approx 160$ km
- **Thin magnetopause**
 - $\Delta M_p \approx 500$ km
- **Generic solar wind input:**
 - southward IMF: $B_X = B_Y = 0$; $B_Z = -8$ nT
 - $V_X = -650$ km/s
 - $V_Y = V_Z = 0$
 - $n = 4$ cm⁻³
 - $P_{th} = 360$ pPa; $T \approx 600$ eV



iPic3D Simulation System

- **3D simulation system:**
 - $4 R_E < x < 11 R_E$
 - $-6 R_E < y < 6 R_E$
 - $-6 R_E < z < 6 R_E$
- **Boundaries:** all open
- **Particles:** initialized with Maxwellian VDFs
- **Parameters:**
 - $T_i / T_e = 10$
 - $m_i / m_e = 25$
 - $350 \times 600 \times 600$ cells
 - $N_e = N_i = 15.750 \cdot 10^9$
 - Domain: $21 \times 36 \times 36 d_j$
 - $\Delta x = \Delta y = \Delta z = 0.06 d_j$
 - $\Delta t = 0.05 \omega_{pi}^{-1}$

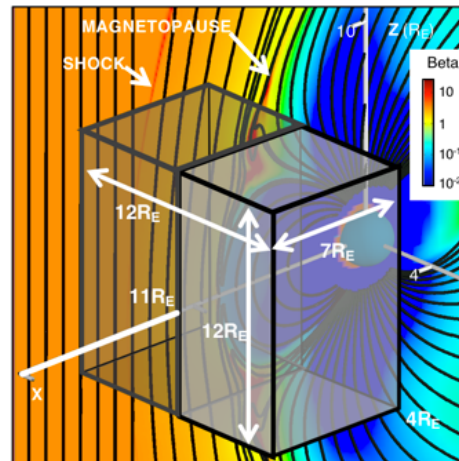


Figure 2: Global MHD and iPic3D Simulation Systems

Large-scale Topology of the Reconnection Region from the PIC Simulation

- The location of the electron diffusion region can be determined by several methods: the perpendicular slippage, the non-ideal terms in Ohm's law, the work $\mathbf{J} \cdot \mathbf{E}$, and the agyrotropy.
- Color contour plots showing the evolution of the perpendicular slippage in the Sun-Earth meridian plane are displayed in the **top panel of Figure 3**; magnetic field lines are superimposed over the contours. They indicate that the initial reconnection region splits very rapidly into two regions which appear to delineate a magnetic island in the 2D plots.

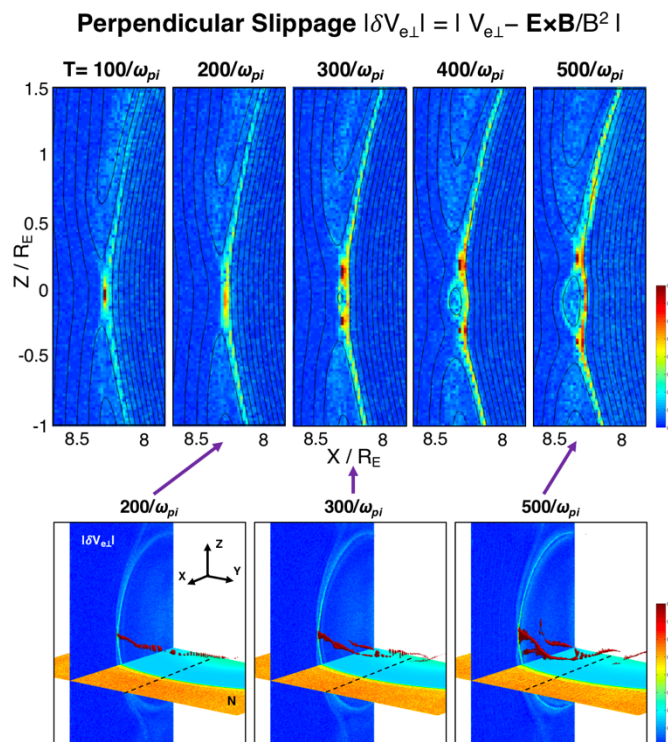


Figure 3: Perpendicular Slippage

- Three-dimensional plots shown in the **bottom panel of Figure 3** display isocontours of a high value of the slippage show that reconnection occurs over most of the dayside magnetopause but spans a limited range in latitude that grows from about 1 to 2 R_E with time. The simulation reveals that the reconnection region has a much more filamentary structure than the solid X-line expected from the extrapolation of 2D models and that it is made up of larger scale structures.

- Tracing field lines through the reconnection filaments shown in Figure 3, reveals that by time $T=500/\omega_{pi}$, two large flux ropes have developed roughly on each side of the meridian plane (**Figure 4**). The dawnward rope is connected to the southern hemisphere while the duskward one is connected to the northern hemisphere. The bottom panel zooms in on a smaller volume of space.

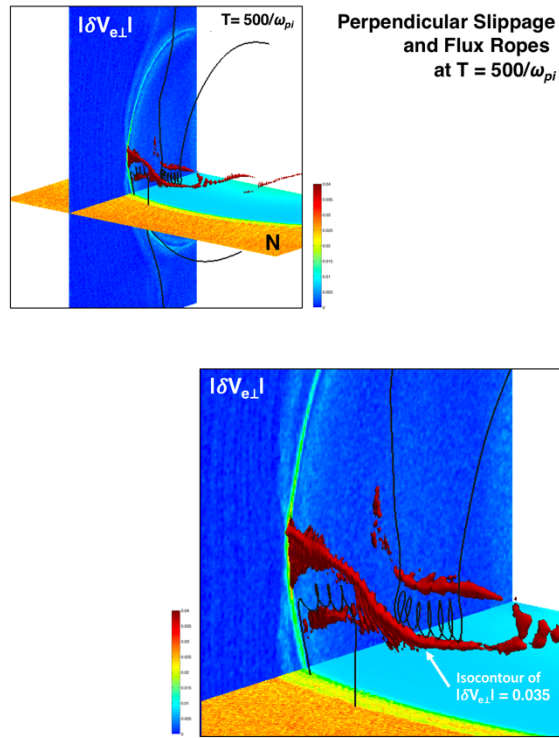


Figure 4: Perpendicular Slippage and Flux Ropes

Electrons and Ions' Parallel Velocities

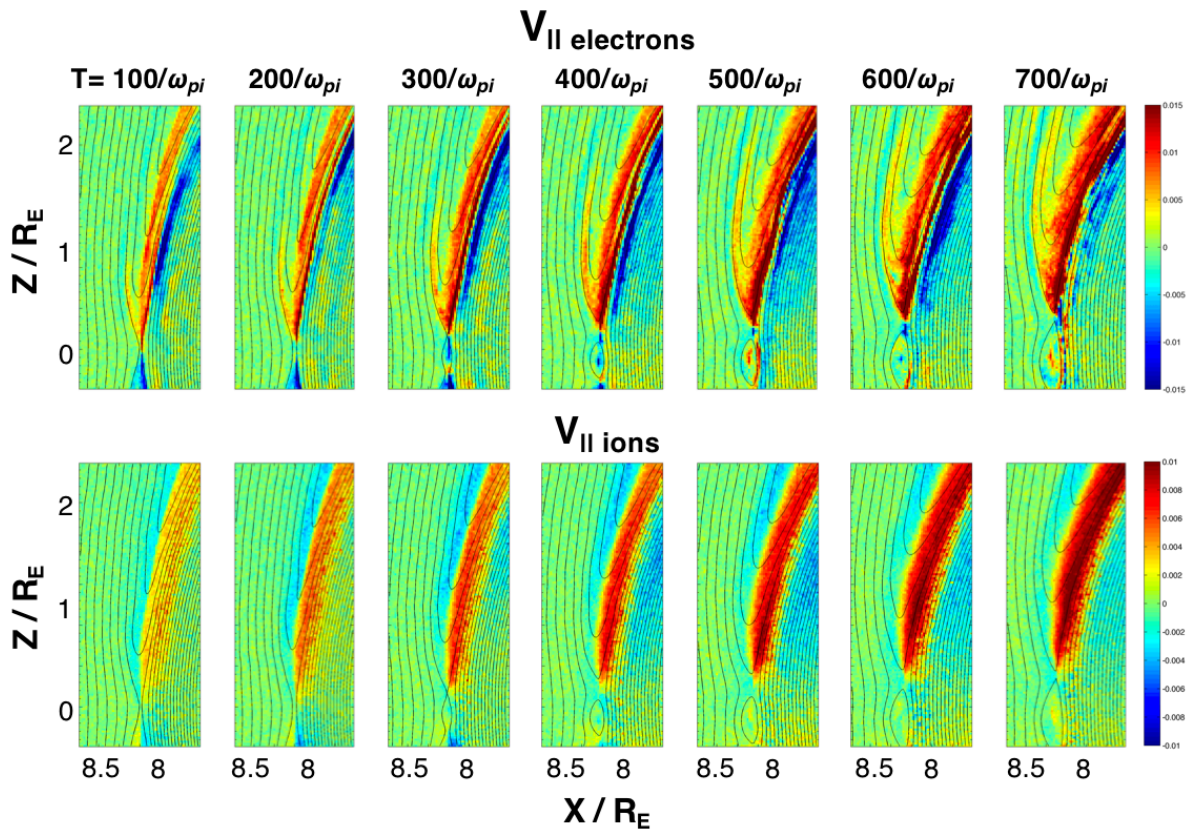


Figure 5: Evolution of the electrons' (top panel) and ions' (bottom panel) parallel velocities. Red and blue contours indicate a $V_{||} > 0$ and $V_{||} < 0$, respectively.

- Color contours are used (Figure 5, top panel) to display the evolution of the parallel electron velocities from time $T=100/\omega_{pi}$ to $T=700/\omega_{pi}$. They are displayed in the Sun-Earth meridian plane. Just a fraction of the northern part of simulation system is displayed.
- The velocity contours show the formation of multiple layers of electrons with significant field-aligned velocities in both the magnetosheath and the magnetospheric boundary layers.
- The fastest electron flows are along the separatrices. They are directed toward the X-line along the magnetosheath separatrix and away from it near the magnetospheric separatrix. Counter streaming electrons are also observed in the region of weak density earthward of the magnetospheric separatrix.
- Ions' parallel velocities (Figure 5, bottom panel) are not as layered as the electrons'. As expected, the ion flow is directed away from the reconnection region on both side of the magnetopause current layer.
- Because of their large gyroradii, the ions' flow is spreading onto regions of closed field lines. This is consistent with the LLBL extending over a region broader than the region bounded by the magnetopause current layer and the magnetospheric separatrix.

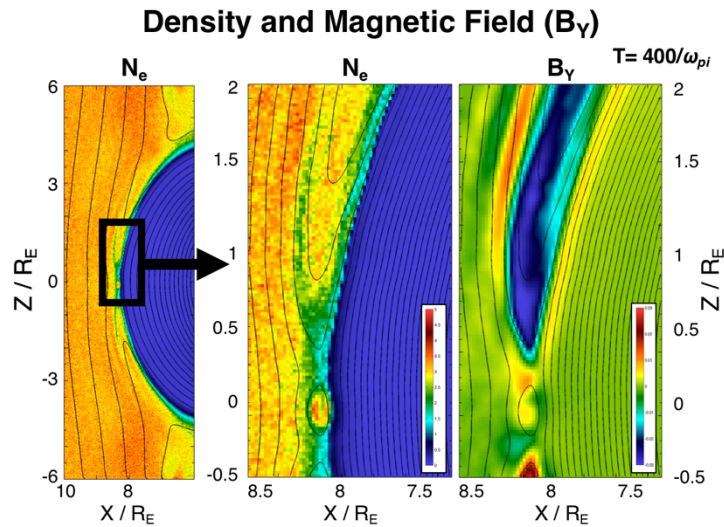


Figure 6: Contour plots of the density and the B_Y component of the magnetic field in the Sun-Earth meridian plane. The $1 \times 2.5 R_E$ area shown in the center and right panels magnify the area delineated by the black rectangle in the left panel.

- A contour plot of the density (Figure 6, middle panel) indicates that high densities are found inside the flux rope and in the exhaust regions at high latitudes, while lower densities are seen in the reconnection regions and along the separatrices. The density gradient is high near the magnetospheric separatrix.
- A plot of the B_Y component of the magnetic field (Figure 6, right panel) shows the formation of a strong Hall-induced magnetic field. While a typical quadrupole Hall structure develops in the early stage of the simulation, plots of the evolution of the B_Y component (not shown here) indicate that the pattern becomes asymmetric as time goes on. The duskward component of the Hall field ($B_Y > 0$) on the magnetospheric side of the current layer shifts to northern latitudes (out of the picture) as a weaker field with $B_Y > 0$ develops on the magnetosheath side (red contours).

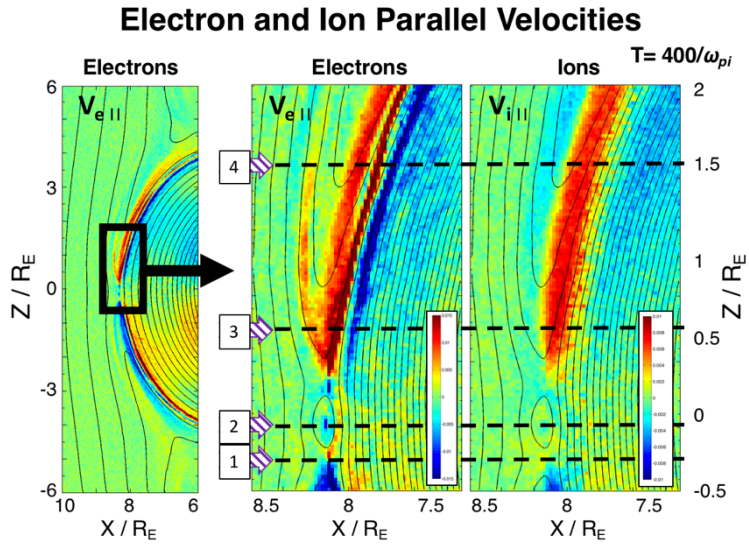


Figure 7: Color contour plots of the ion and electron parallel velocities (right and center panels) for time $T = 400/\omega_{pi}$. The contours are traced in a $1 \times 2.5 R_E$ area of the Sun-Earth meridian plane, which is shown by the black rectangle displayed in the left panel. Red and blue contours indicate a $V_{||} > 0$ and $V_{||} < 0$, respectively.

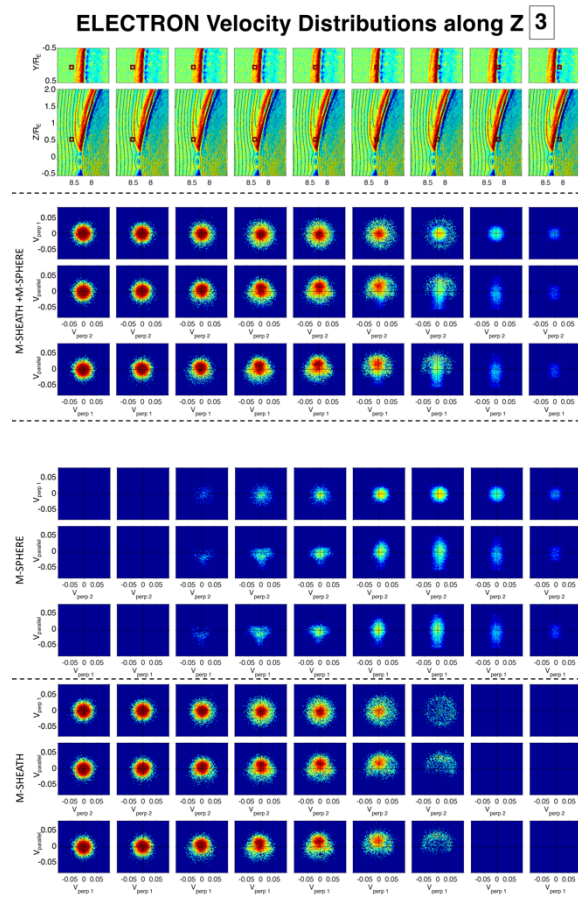
- Figure 7 shows the 4 paths that were used to follow the evolution of the velocity distribution functions through the MSBL and LLBL. They are indicated by the boxed numbers displayed on the left of the center panel showing the electron parallel velocities.

Origins and Evolution of the Electron and Ion Populations

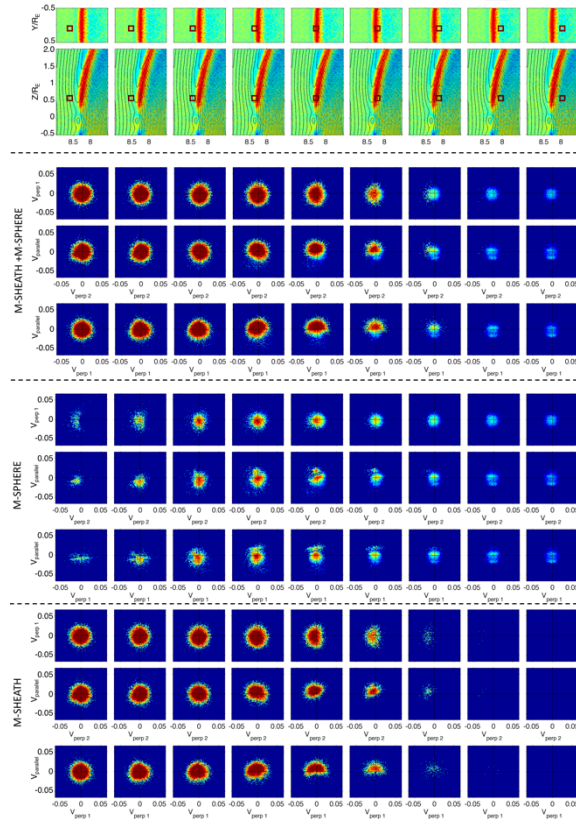
We systematically examined electron and ion velocity distributions along the 4 paths described in Figure 7. As an example, we display below the results for **Path 3** which cuts the magnetopause boundary layers above the flux rope. **Plate 1** shows the electron distributions and **Plate 2** the ion distributions.

The simulation lets us keep track of the origin of the particles. This allows us to separate the two populations and determine the contributions of the magnetosheath and magnetospheric populations to the velocity distribution functions.

Path 3



ION Velocity Distributions along Z 3

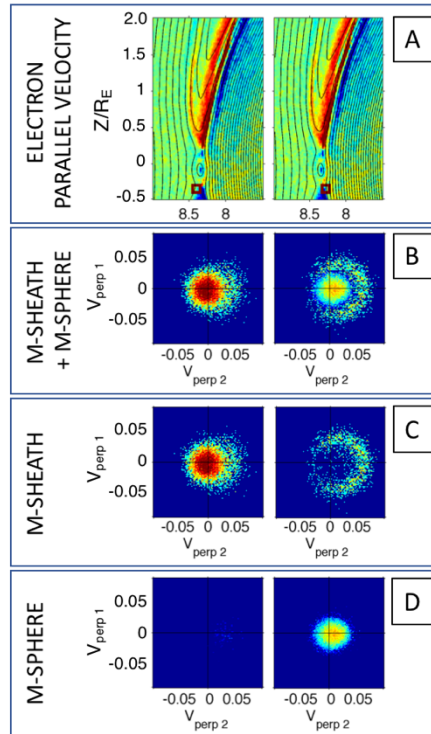


Each plate is organized as follows:

- The top 2 rows show the different locations of the cube used to collect the particles' velocities. The traces of the cube are displayed in the X-Y (top) and X-Z (bottom) plans and superimposed over the parallel velocities in these plans.
- The next 3 rows shows the distribution of the velocities of the entire population contained in the cube, i.e. particles with both magnetospheric and magnetosheath origins. The distributions are displayed V_{perp1} vs V_{parallel} (bottom) and V_{perp2} vs V_{parallel} (middle) and vs V_{perp1} (top). The direction of V_{perp1} is defined by $(\mathbf{b} \times \mathbf{v}) \times \mathbf{b}$, where \mathbf{b} and \mathbf{v} are unit vectors of \mathbf{B} and \mathbf{V} ; V_{perp2} is defined by $(\mathbf{b} \times \mathbf{v})$.
- The following 3 rows shows the velocity distributions of the particles of magnetospheric origin.
- The bottom 3 rows display velocity distributions of particles from magnetosheath origin. Partial distributions use the same format as the one used to display the result for the entire population.

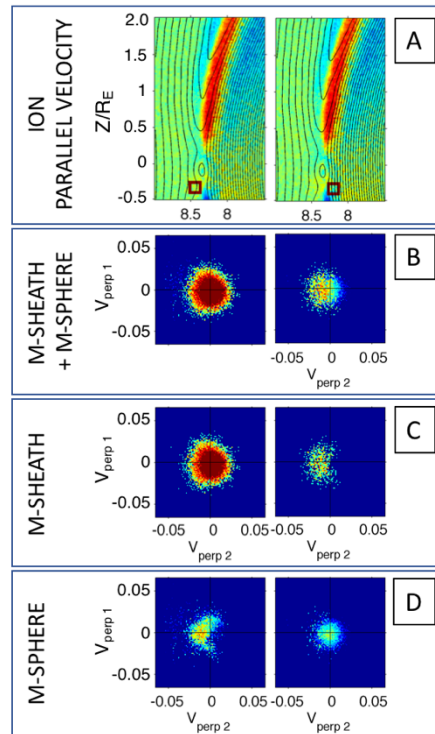
Considering the large amount of information produced by the analysis of the distributions, we highlight a few interesting features revealed by the distributions along the 4 paths described in Figure 7.

Path 1



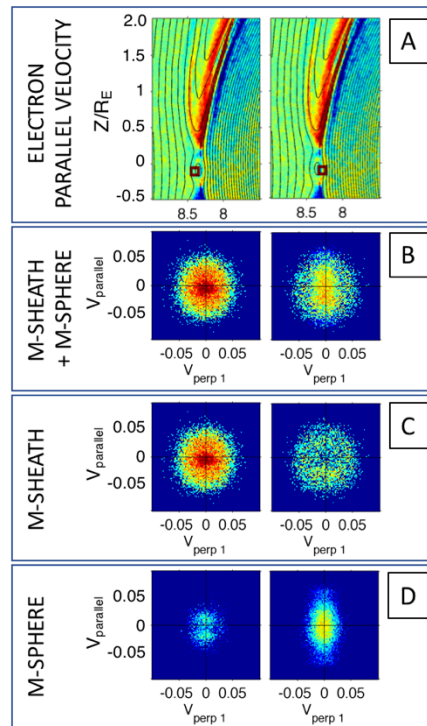
- **Panel A:** Color contours of the electrons' parallel velocities. The small boxes located in the flux rope (left column) and near its magnetospheric edge (right column) show the location of the cube used to calculate the distribution functions displayed below.
- **Panel B:** Velocity distribution of all the electrons (i.e. originating from both the magnetosheath and the magnetosphere) located in the small boxes shown in Panel A
- **Panels C and D:** Velocity distribution of electrons of magnetosheath and magnetospheric origin respectively

Electrons: The expected crescent shaped distribution observed when crossing the electron diffusion region results solely from the meandering of the magnetosheath population in that region (Panel C). The core of the distribution consist of magnetospheric electrons that are accelerated in the parallel direction (Panel D).



Ions: The panels above have the same format as the previous panels showing electrons. Crescent shaped distributions are observed on each side of the magnetopause current layer. Magnetosheath ions contribute to the one observed in the magnetospheric boundary layer (Panel C) and vice versa: magnetospheric ions contribute to the one observed in the magnetosheath boundary layer.

Path 2



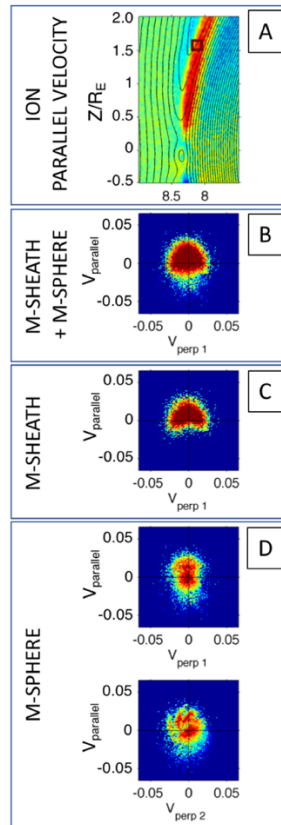
Flux rope: Plots of velocity distribution functions inside the flux rope show that both magnetosheath and magnetospheric electrons are present. However, the magnetosheath component is more strongly heated (Panel C). A strong magnetospheric field-aligned component is observed just outside the rope (Panel D).

Path 3 (see Plates 1 & 2)

Electrons: Velocity distribution functions found near the magnetosheath separatrix and the current layer show that the electron population of magnetosheath origin is composed of a component flowing toward the reconnection region and a smaller, heated outflow component. The distribution becomes closer to a Maxwellian on the magnetospheric side of the current layer. Crossing the magnetospheric separatrix, the magnetosheath population exhibits a crescent-like shape, but only in the outer part of it. The electron population of magnetospheric origin found near the magnetosheath separatrix is composed of two outflows: an accelerated field-aligned component and a heated transverse one.

Ions: Magnetosheath ions form clear D shaped distributions in the V_{perp1} versus V_{parallel} plots, while the magnetospheric ones show some structures and beams.

Path 4



- Panel A:** As expected, color contours of the ion parallel velocities indicate that the ions flowing away from the reconnection site with $V_{\parallel} < 0$ (blue contours) since the IMF $B_z < 0$ in the MSBL and with $V_{\parallel} > 0$ (red contours) since the magnetospheric $B_z > 0$ in the LLBL. The yellowish layer between the two regions is the main magnetopause current layer marked by the reversal of the magnetic field. The small box located at the edge of the LLBL at $Z = 1.5 R_E$ shows the location of the cube used to calculate the distribution functions displayed below.
- Panel B:** Velocity distribution of all the ions plotted $V_{\text{perp}1}$ vs V_{parallel} . A prominent D shape expected for reconnection outflow distributions is observed. Only ions with velocities above a cut-off field aligned speed of $\mathbf{V}_{\text{HT}} \cdot \mathbf{b}_{\text{mag}}$ (with $|\mathbf{V}_{\text{HT}}| = E_t/B_n$) can cross the current layer.
- Panel C:** Velocity distribution of magnetosheath ions only. It shows a "cleaner" D shape than the one observed for all the ions (Panel B) as it is predicted for magnetosheath ions transmitted into the LLBL [Cowley, 1982].
- Panel D:** Velocity distribution of magnetospheric ions only. It shows that relatively slow ions are flowing toward the reconnection site ($V_{\parallel} < 0$), some being reflected ($V_{\parallel} > 0$) and forming structures reminiscent of stochastic resonances near thin current sheets.

Summary

We present the results of one of the first regional PIC simulations encompassing a large volume of the dayside magnetosphere ($7 \times 12 \times 12 R_E$). The implicit PIC code (iPic3D) was initialized from a global MHD state of the magnetosphere.

1. Plots of the evolution of the perpendicular slippage show the formation of a magnetic flux rope with a cross section that grows to about $1 R_E$ within $200 / \omega_{pi}$.
2. Three-dimensional plots of the perpendicular slippage indicate that reconnection occurs over most of the dayside magnetopause but spans a limited range in latitude. The reconnection region appears to have a much more filamentary structure than the X-line expected from the extrapolation of 2D models.
3. Plots of parallel electron velocities show the formation of multiple layers of electrons with significant field-aligned velocities; the stronger electron flows are toward the X point along the magnetosheath separatrix and away from it along the magnetospheric separatrix.

We use a new technique to distinguish the origin of the electrons in the simulation. Separating the magnetosheath component from the magnetospheric component of the electron population when analyzing velocity distribution functions reveals the following:

1. The expected crescent shape observed when crossing the electron diffusion region results solely from the meandering of the magnetosheath population in that region. The core of the distribution is made by magnetospheric electrons that are accelerated in the parallel direction.
2. Plots of velocity distribution functions inside the flux rope show that both magnetosheath and magnetospheric electrons are present, the magnetosheath component being strongly heated.
3. Above the flux rope, velocity distribution functions found near the magnetosheath separatrix and the current layer show that the electron population of magnetosheath origin is composed of a component flowing toward the reconnection region and a smaller heated outflow component. The electron population of magnetospheric origin found near the magnetosheath separatrix is also composed of two outflows: an accelerated field-aligned component and a heated transverse one.
4. At higher latitudes, velocity distribution functions show features similar to those seen in (3), but with more pronounced D-shaped distributions in the V_{perp1} versus $V_{parallel}$ plots.